UNIVERSITAT POLITÈCNICA DE VALÈNCIA

ESCUELA TÉCNICA SUPERIOR INGENIERÍA INDUSTRIAL VALENCIA

INDUSTRIAL ENGINEERING MASTER THESIS

CHARACTERISATION OF ZIRCONIA-SILICON CARBIDE CERAMICS PROCESSED BY SPS

AUTHORESS AUDREY CORMERY

SUPERVISOR: BENAVENTE MARTINEZ, RUT

SUPERVISOR BORELL TOMAS, MARIA AMPARO

Academic year: 2020-21

Index

Acknowledgements

I would like to acknowledge everyone who played a role in my academic accomplishments in doing this research project abroad, at the UPV.

First of all, my teachers, Borrell Tomás, María Amparo and Benavente Martínez, Rut for giving me a project subject at the last minute and welcomed me with open arms into their team. I learned a lot, thanks for guiding me in this work, for the attention and for the knowledge they gave me, with so much patience and devotion.

Secondly, each person I worked with, at UPV, at ITM, and everyone who provided me help in doing research or experiences, and without who I would have not be able to understand everything.

Finally, Manon, my friend and roommate for helping me finding my supervisor, and for sharing together our doubts and questions during this time in Valencia.

List of tables

List of equations

List of figures

Abstract

This final master's degree project aims to address the development of ceramic composite materials used in the aerospace sector to act as thermal barriers in gas turbines. The requirements of these materials are severe, since they have to resist high temperatures in abrasive environments protecting the metal blades.

For this purpose, ZrO_2 based ceramic composites reinforced with different proportions of SiC and processed by Spark Plasma Sintering (SPS) have been used. As matrix of the composite, tetragonal zirconia doped with 4% mol of yttria (4YTZP) was used, a material widely studied for its low thermal conductivity, high tenacity, high hardness and high coefficient of thermal expansion. As reinforcement, silicon carbide (SiC) was selected for its good mechanical properties and its ability to inhibit crack propagation, thus increasing its toughness.

The different 4YTZP-SiC composites obtained have been sintered in vacuum by the non-conventional Spark Plasma Sintering technique at different temperatures (1300, 1350 and 1400 ºC), with a uniaxial pressure of 80 MPa, a heating ramp of 100 ºC/min and a stay of 5 min.

Once the composites have been obtained, they have been characterised by X-ray diffraction. Their microstructure has been studied using SEM techniques and their mechanical properties have been analysed using microhardness and toughness. Finally, to study the behaviour of these materials in abrasive environments, scratch tests have been carried out in which the load and depth of penetration have been varied.

Key words: stabilised zirconia, SiC, SPS, microstructure, mechanical properties, scratch.

Resumen

En el presente trabajo fin de máster se pretende abordar el desarrollo de materiales compuestos cerámicos empleados en el sector aeroespacial que actúen como barreras térmicas en turbinas de gas. Los requerimientos de estos materiales son severos, ya que han de resistir altas temperaturas en ambientes abrasivos protegiendo los álabes metálicos.

Para ello se han empleado composites de cerámicas base ZrO_2 reforzadas con diferentes proporciones de SiC y procesadas mediante Spark Plasma Sintering (SPS). Como matriz del composite se empleó circona tetragonal dopada con un 4% mol de itria (4YTZP), un material ampliamente estudiado por su baja conductividad térmica, alta tenacidad, alta dureza y alto coeficiente de expansión térmica. Como refuerzo se seleccionó carburo de silicio (SiC) por sus buenas propiedades mecánicas y su capacidad de inhibición en la propagación de las grietas, aumentando así su tenacidad.

Los diferentes composites 4YTZP-SiC obtenidos se han sinterizado en vacío por la técnica no-convencional de Spark Plasma Sintering a diferentes temperaturas (1300, 1350 y 1400 °C), con una presión uniaxial de 80 MPa, una rampa de calentamiento de 100 °C/min y una estancia 5 min.

Una vez obtenidos los composites, se han caracterizado mediante difracción de rayos X. Se ha estudiado su microestructura mediante técnicas de FESEM y se han analizado sus propiedades mecánicas mediante microdureza y tenacidad. Por último, para estudiar el comportamiento de estos materiales en ambientes abrasivos, se han realizado ensayos de rayados en los que se ha variado la carga y la profundidad de penetración.

Palabras clave: circona estabilizada, SiC, SPS, microestructura, propiedades mecánicas, scratch.

Resum

En el present treball fi de màster es pretén abordar el desenvolupament de materials compostos ceràmics empleats en el sector aeroespacial que actuen com a barreres tèrmiques en turbines de gas. Els requeriments d'aquests materials són severs, ja que han de resistir altes temperatures en ambients abrasius protegint els àleps metàl·lics.
Per a això s'han emprat composites de ceràmiques base ZrO_2 reforçades amb diferents proporcions de SiC i processades mitjançant Spark Plasma Sintering (SPS). Com a matriu del composite es va emprar circona tetragonal dopada amb un 4% mol de itria (4Y-TZP), un material àmpliament estudiat per la seua baixa conductivitat tèrmica, alta tenacitat, alta duresa i alt coeficient d'expansió tèrmica. Com a reforç es va seleccionar carbur de silici (SiC) per les seues bones propietats mecàniques i la seua capacitat d'inhibició en la propagació de les clivelles, augmentant així la seua tenacitat.
Els diferents composites 4YTZP-SiC obtinguts s'han sinterizado en buit per la tècnica no-convencional de Spark Plasma Sintering a diferents temperatures (1300, 1350 i 1400 °C), amb una pressió uniaxial de 80 MPa, una rampa de calfament de 100 °C/min i una estada 5 min.

Una vegada obtinguts els composites, s'han caracteritzat mitjançant difracció de raigs X. S'ha estudiat la seua microestructura mitjançant tècniques de FESEM i s'han analitzat les seues propietats mecàniques mitjançant microdureza i tenacitat. Finalment, per a estudiar el comportament d'aquests materials en ambients abrasius, s'han realitzat assajos de ratllats en els quals s'ha variat la càrrega i la profunditat de penetració.

Paraules clau: Circona estabilitzada, SiC, SPS, microestructura, propietats mecàniques, escratx.

1. Introduction and work objectives

Nowadays, it is necessary to have materials with high properties, to satisfy a high level of requirements in various fields. Because of it, also arises the need of creating new technics to sinter higher properties materials.
For thousands of years, ceramics have been employed in daily life applications such as dishes, dental applications, … because of its high hardness, high temperature resistance, and also its inert nature. However, these properties are not enough for today's requirements, that is why a new generation of ceramics, called "advanced ceramics" are processed. These materials, with a high purity and a high density are processed from powders. They are designed for specific applications, expanding especially in industrial sectors.
They are called "advanced" materials, because in addition to classical ceramics properties, they succeed in having better optical, magnetic and mechanical properties, thanks to the non-conventional sintering process leaded: the Spark Plasma Sintering.
The materials employed as TBCs, must continue to improve their properties. Even the zirconia based ceramics might enhance their properties to allow the structural components to have a longer lifetime. Thus, the present work will focus on the development of zirconia-based materials, with addition of SiC processed by SPS, to obtain ceramic with high properties, with a shorter processing time. According to (A. Borrell, 2020), adding SiC has been shown acting as crack inhibitor.

The aim of this work is to study a composite material with improved properties, capable of acting as a self-sealing agent for cracks, which are generated in components subject to sudden changes in temperature, which deteriorate and shorten their useful life.
In order to carry out the main objective of this work, a series of specific objectives have been set, which are indicated below:

- Preliminary study of materials, actual work on the subject and needs in this field
- Study of a process to obtain the densified composite by means of the rapid sintering technique using a pulsed electric field (SPS)
- Study and evaluation of the properties of zirconia-based composites with additions of 15 and 20% by weight of SiC
- Study of the crack inhibitor capacity/functionality of composites developed with the addition of SiC by the Scratch test and SEM observations

2. Actual problematics

The Thermal Barrier Coatings (also called TBCs) first appeared at the end on the 40's. (Miller, CURRENT STATUS OF THERMAL BARRIER, 1987) They are mostly employed in turbines, in order to create a protective layer between the warm gas in the motor and the structural metallic component. This coating has to resist to temperature changes, up to 1000°C between to cycles which are creating cracks on the coating while cooling. Because of it, high tension areas are created because of the expansion coefficient differences. The lifetime of the device is therefore clearly reduced.

From the middle of the 70's, the TBCs are more employed, but what started the modern TBCs era is the use of YSZ/NiCrAlY on the J-75 turbine blades (Figure 1), it was processed by the NASA and tested in a research gas turbine engine (Miller, Thermal Barrier Coatings for Aircraft Engines: , 1997).

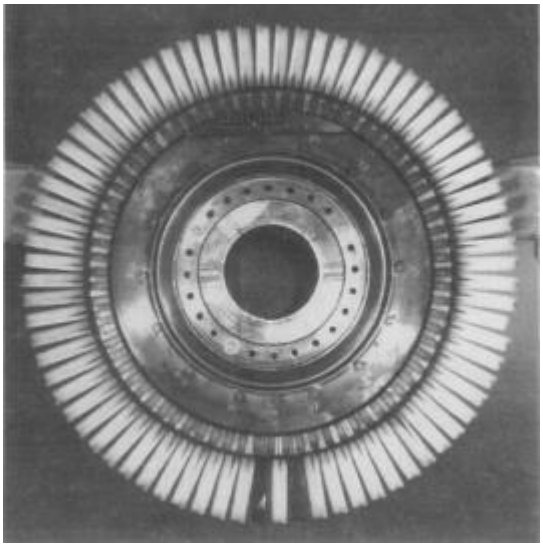

Figure 1: YSZ/NiCrAlY coated turbine blades.

In order to enhance the lifetime of the TBCs, zirconia-stabilized based ceramics sintered by Spark Plasma Sintering, in which SiC is added to act as a crack inhibitor, is currently studied.

The main mechanisms creating defects on the TBCs are the following:

- Tensions due to thermal expansion differences
- Oxidation of the structural metal that leads to an immediate change of the component
- Composition, problems of homogeneity, microstructure of the material

3. State of the art

a.Materials studied

i.Zirconia

Zirconia based ceramics are already widely employed many fields such as in the biomedical field, for piezoelectric components, or thermal barriers,…. The zirconia dioxide (ZrO_2) is a white powder which can be processed to become a ceramic with ionic bonds. Thanks to its interesting properties (Figure 2), such as a high toughness and a high melting point (around 2700°C), added to the safety of a chemically inert material, zirconia is a very promising material, even in other fields.

Properties (unit)	ZrO_2
Melting point (°C)	2,720
Thermal conductivity (W/mK)	2
Electrical resistivity (Ω cm)	$>10^{11}$
Vickers hardness (Hv)	1,200–1,300
Toughness (MPa $m^{1/2}$)	5.4
Strength (MPa)	850–1,500
Specific heat (J/kg K)	400
Density (kg/m^3)	5,680

Figure 2 : Physical and mechanical Zirconia properties.

Depending on the temperature, zirconia has various phases presented in the Figure 3.

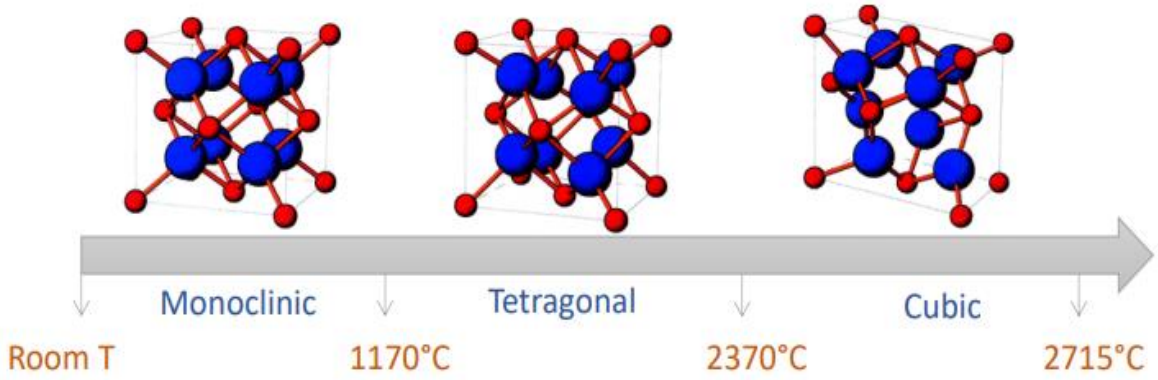

Figure 3: Phases of the Zirconia depending on the temperature.

The monoclinic phase is present from room temperature until 1170°C, then until 2370°C the major phase is tetragonal and finally from 2370°C to 2715°C, the phase is cubic. Depending on the temperature, structural and mechanical properties are different. The main issue with zirconia is the transformation from the tetragonal to the monoclinic phase during the cooling, it leads to a volume increase of around 4%, creating weakness in the microstructure and thus a brittle material after a few heating/cooling periods. (Kelly, 2007)

Tetragonal and cubic phases present the best properties, nevertheless they cannot be used with pure zirconia, indeed, zirconia can be stabilized thanks to several oxide such as magnesium (MgO), cerium (CeO_2) or yttrium (Y_2O_3). (Borrell Tomás & Salvador Moya, 2018)

ii.Y-TZP: yttria-doped tetragonal zirconia polycrystal

At room temperature, ZrO_2 is not stable. The transformation from tetragonal to monoclinic (t→m) is non diffusive and leads to a volume increase of 4%. During the cooling of the processed ceramics, the tensions created by this variation can create cracks leading to the breaking of the ceramic.

The Zirconia's stable phase at room temperature is the monoclinic, but the phases showing the best mechanical and structural properties are the cubic and tetragonal ones (Figure 4). To be employed as a structural ceramic, the transformation t→m during the cooling might be avoided. By adding 4% of Yttria (Y_2O_3), it is possible to obtain tetragonal zirconia polycrystals at room temperature, composed of tetragonal grains with a size order of nanometres. (Borrell Tomás & Salvador Moya, 2018) (Kelly, 2007)

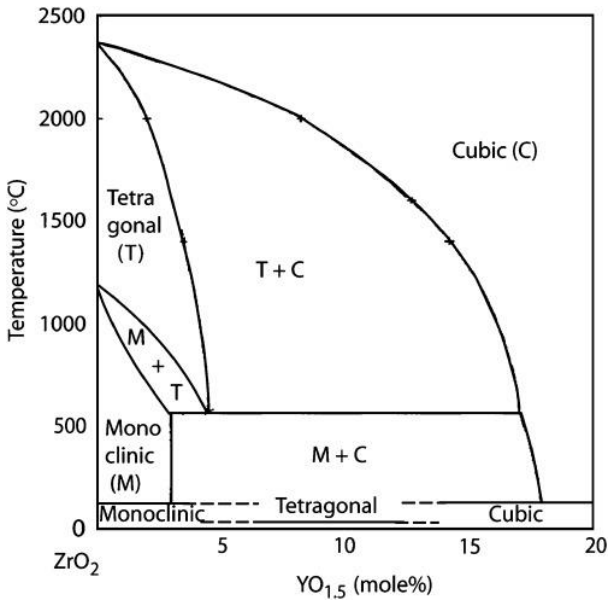

Figure 4: phases diagram of zirconia.

Various t-phase stabilized zirconia can be produced, the most interesting remains being the TZP one. Due to the change between the tetragonal phase and the monoclinic phase, the resistance against crack propagation can be enhanced.

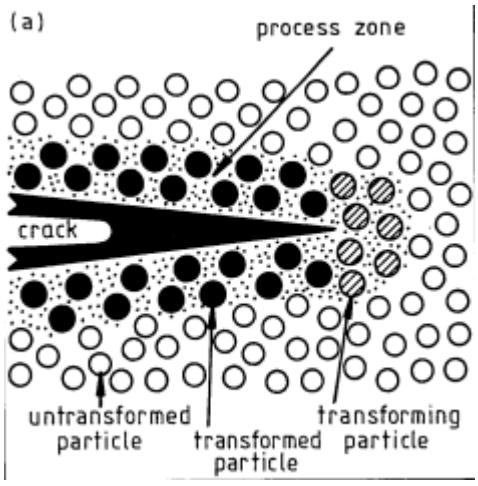

Figure 5: Toughening mechanism and crack propagation (Butler, 1985).

In the Figure 5 is shown how the toughening transformation happens. First the stress field in front of the crack tip gives enough energy to allow the tetragonal particles to change into monoclinic phase zirconia particles (transforming particle), instantly, the transformation happens, and a volume increase is observed (t→m transformation). This volume change implies residual compressive tensions reducing the magnitude of the tensile forces around the crack by dissipating the energy normally used to propagate the crack. (Butler, 1985)

In the Table 1, one can found the values obtained for classical properties once the zirconia is stabilized by 4% of Yttria.

Table 1 : 4YTZP physical/mechanical properties (A. Borrell, 2020).

Properties of the powder TZ4YS	
Chemical composition	96 % ZrO_2, 4 % Y_2O_3
Specific density (g cm-^{3})	6.05
Grain size (nm)	70
Superficial area ($m^2\ g^{-1}$)	7.00
Porosity (%)	< 0.10
Melting point (°C)	2380
Elasticity modulus (GPa)	210
Hardness Vickers (HV)	1250
Critical toughness, K_{IC} (MPa $m^{1/2}$)	1-2
Thermal expansion coefficient ($10^{-6}\ K^{-1}$)	11.50

iii.SiC

Silicon carbide (SiC) is one of the most popular ceramic material in the industry for a long time. Thanks to its electrical and mechanical properties, it is widely employed as a structural part. SiC particles added in a YTZP matrix allow to produce ceramics with better mechanical properties due to their good thermal shock resistance despite their poor sinterability and low fracture toughness. (A. Borrell, 2020)

Fig. XX shows the phase diagram between silica and carbon, there is not only liquid phase, indeed around 2700°C, SiC is transformed into graphite and vapor phase mainly made of Si. (Figure 6)

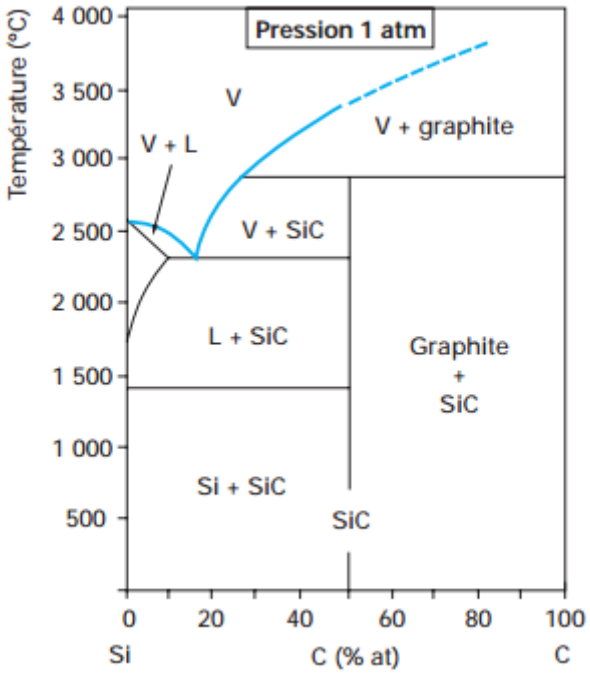

Figure 6: Phase diagram of SiC (RAYNAUD, 2007).

The bond Si-C is not only covalent, because of the electronegativity difference between Si and C. This bond provides the high mechanical and structural properties. (RAYNAUD, 2007)

Moreover, SiC is very interesting because of its semi conductive properties. In this project the sintering process employed required a current flow into the sample, thanks to SiC it is possible.

b.Processes

i.Conventionnal sintering

The sintering is a process in which a compacted powder is transformed into a dense and resistant ceramic. The powder is heated at a temperature high enough to activate transformation mechanism,

but not too high to avoid the melting, to obtain a densified material. (Borrell Tomás & Salvador Moya, 2018) By increasing the density, the porosity is less important, leading to better mechanical properties. This sintering could be processed either in liquid or solid state. With our materials, solid state sintering can be employed. The driving force of the sintering process is the decrease of the system's energy. The solid-vapor interphases (porosity) are more energetic than the soli-solid ones (grain boundary). In order to decrease the system's energy, two ways are possible under temperature effect: (Bichaud., 2016)

- Decreasing of the interfacial area by the particle's coalescence.
- The solid-vapor interface (high energy free surface) is changed into a solid-solid interface (low energy grain boundary) by joining grains together, with or without densification. (Borrell Tomás & Salvador Moya, 2018)

ii.Spark Plasma Sintering

Usually, the conventional sintering time and temperature are high, allowing the increasing of the particle grain size. In case of SPS, ceramic composites show high mechanical properties while keeping small grain sizes and good densification, because the processing time is short. (A. Borrell, 2020)

The SPS principle is very similar to the conventional hot-pressing process. A uniaxial pressure is applied on a mould filled with powder. The main difference between these two is that contrary to hot pressing, the heat applied on the mould is not coming from an external source but from a current flowing at the surface of the sample (at least) and in the sample. The **Erreur ! Source du renvoi introuvable.** shows the global SPS installation. The processing time, the heating rate, the length of the pulses, and the voltage are parameters which can modify the sintering.

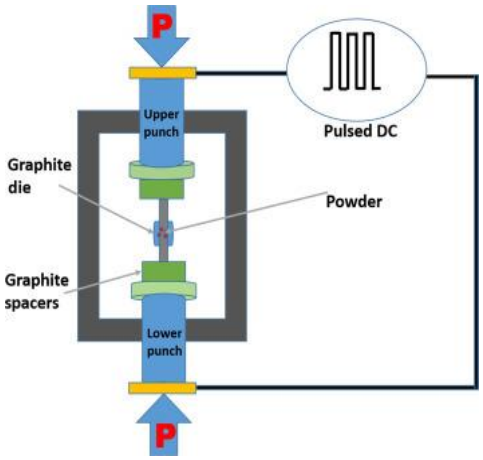

Figure 7 : SPS equipment

A pulsed current is often employed to control in an easier way the temperature of sintering. Indeed, the powder is put in a mould covered by graphite. Graphite is employed as a coating because the mould needs to be conductive and resist to high temperature and pressure. (ESTOURNES, 2006) The name of the technic "spark plasma sintering" comes from the plasma shock between the grains. Thanks

to this plasma, the grain surface is cleaned from all impurities, and the grain surface can easily transfer the energy. (ESTOURNES, 2006)
Despite the change in temperature and processing time, one main advantage of this technique is that the temperature gradient inside the sample is much lower than with conventional sintering, due to the internal heating, allowing the sample to be more homogeneous.

Classic values for SPS parameters are the following:

- Pressure between 50 and 100 MPa (for a graphite mould, the pressure will depend on the material employed for the mould)
- Heating rate up to 600°C·min^{-1}
- Pulse of around ~10 ms with on-off cycles of 2-5 ms
- Maximum values of 10 000 A and 10 V.

The densification of the green bodies happens during 4 main steps: 1) under vacuum,2) pressure, 3) heating,4) cooling. During the first step, the system is under vacuum in order to eliminate all the air present on the system. Then the pressure applied starts to compact the powder, and the heating continues.

4. Experiments

The main goal of this project is to characterize ceramics obtained by SPS. Different compositions and various sintering temperature have been used to see the impact on the mechanical properties of the sintered samples.

Three different samples studied, and their given names are gathered on the Table 2.

Table 2 : Samples and given names

	Materials		
Sintering temperature	4YTZP	4YTZP/15SiC	4YTZP/20SiC
1300°C	4YTZP-1300°C Z-1300°C	4YTZP/15SiC-1300°C Z15C-1300°C	4YTZP/20SiC-1300°C Z20C-1300°C
1350°C	4YTZP-1350°C Z-1350°C	4YTZP/15SiC-1350°C Z15C-1350°C	4YTZP/20SiC-1350°C Z20C-1350°C
1400°C	4YTZP-1400°C Z-1400°C	4YTZP/15SiC-1400°C Z15C-1400°C	4YTZP/20SiC-1400°C Z20C-1400°C

The following parts detail the experiments lead and how the data were obtained.

a.Composition and preparation of the samples

i. Compaction and SPS

Powders with the needed composition were placed in the graphite die with an inner diameter of 20 mm and uniaxially pressed at 30 MPa. The next step was to put them in the SPS apparatus HP D25/1 (FCT Systeme GmbH, Rauenstein, Germany) under low vacuum (1 Pa) and sintering temperatures from 1300°C to 1400°C, and a constant and uniaxial compaction pressure of 80 MPa. Tests were carried out with a heating rate of 100 °C·min^{-1} and 5 minutes of dwelling time at maximum temperature.

ii. Embedding and Polishing

To be studied, the samples need to be embedded, so they are easier to manipulate. They are embedded in a transparent resin, initially found as a white powder. The powder (and the sample) is heated at 180°C during 3 m and 30 s and is cooled for 6 min. The pressure applied is 350 bar.

To study the hardness for instance, the sample needs to have a very flat surface. To obtain a flat surface, 6 polishing steps are required, with discs having various grain size (Figure 8) and lubricated with the parameters in the Table 3.

Table 3: Polishing steps.

Grain	Lubricant	Load applied	Velocity	Time
40 µm	Water	10 N	100 rpm	1 min
20 µm	Water	10 N	100 rpm	1 min
10 µm	Water	10 N	100 rpm	1 min
MD Largo	6 µm	20 N	150 rpm	10 min
MD Plus	3 µm	20 N	150 rpm	8 min
MD Nap	1 µm + Oil	10 N	150 rpm	8 min

Figure 8: polishing plates.

b.Hardness Vickers

Hardness is determined as the resistance of a material to local plastic deformation achieved from indentation of a predetermined geometry indenter onto a flat surface under a predetermined load. (Faraji, Kim, & Kashi, 2018)

The following explanations show one model of hardness device, it can differ with the brand of the apparatus and the model.

To process the micro hardness measurement, various indenter can be employed depending the properties studied. This micro-hardness measurement has been performed by a Vickers indenter. It is pyramidal shaped diamond with a square base and angles of 136°. A known load is applied on the tip, and the print left by it on the material leads to the hardness using the Equation 1.

$$H_v = \frac{2F \,.\, \sin\frac{136°}{2}}{9.80665 . d^2}$$

Equation 1: Vickers hardness

With F the load applied in Newton, and d the mean value of the diagonal length (m) measured as shown on the Figure 9 explaining the measurement principle.

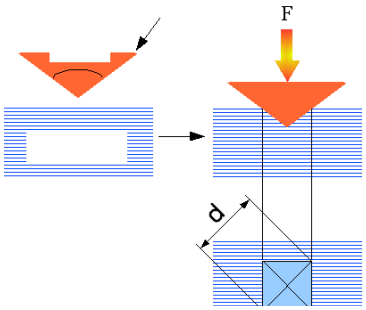

Figure 9: Vickers micro hardness measurement principle (Moustabchir, 2008)

The test was processed ten times for each sample in order to get representative values, with a load of Hv 1.0 during 6 s. The pictures on Figure 10 are obtained thanks to pictures taken by an optical microscope (Figure 11). The diagonal length can be easily measured thanks to a picture treatment software.

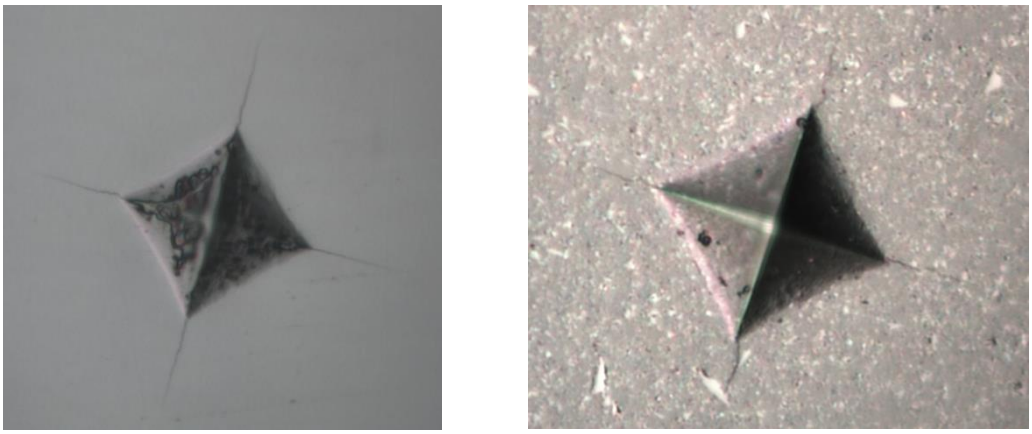

Figure 10: (left) : Z – 1350°C – x400; (right) Z15C – 1350°C – x400

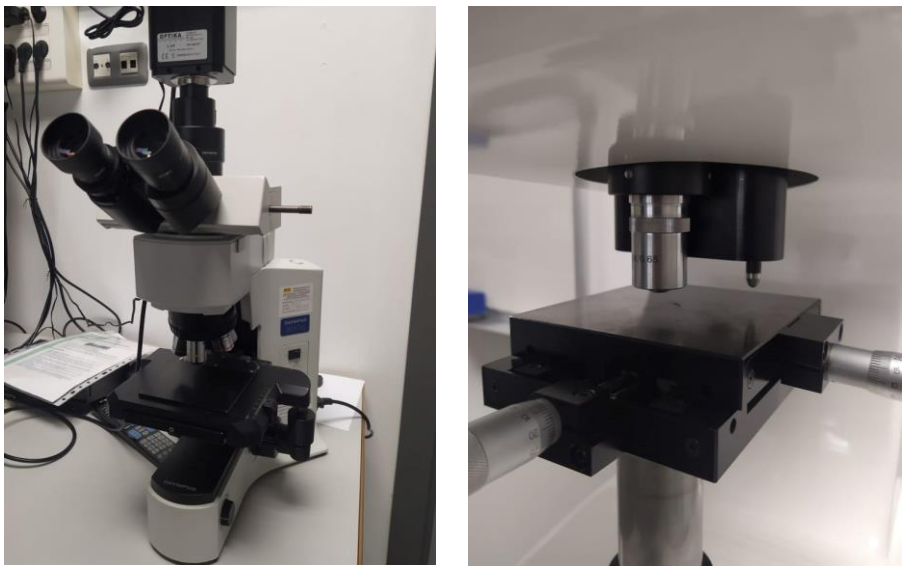

Figure 11: (left) Micro hardness / microscope device “Olympus ”, (right) zoom on the microscope and Vickers indentator.

c.Fracture toughness

The fracture resistance is usually characterized by the mode I fracture. The K_{Ic}, that is the plain strain fracture toughness value comes from the linear elastic fracture mechanism. Indeed, K_{Ic} is the magnitude of the stress field in the crack tip region.

KIc is generally thought of as the lower limiting value of fracture toughness in the environment and at the speed and temperature of the test.
To measure the fracture toughness, the often used, Vickers indention fracture (VIF) toughness test can be used. The measurement is based on the crack length measurement, with a known loading value. The method consists of measuring the length of the cracks starting at the edges of the tip print. The crack length is in inverse proportion to the toughness, one can determine KIc by measuring it. This method is efficient and easy to process, only a small amount of material is needed, and the sample preparation time is short.

Two different kinds of cracks can be created during the VIF, therefore, it is necessary to choose the right model corresponding to the crack profile to make the most accurate calculations. The two crack models are the presented in the Figure 12.

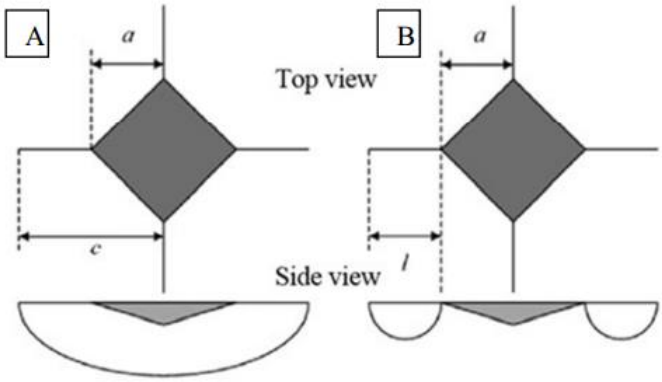

Figure 12: Cracks emanating from VIF, A) radial-median crack and B) Palmqvist crack.

By having the values of a and c for the materials studied, it is possible to determine the crack profile, even without seeing it. If the a/c value is lower than 2.5, the crack will follow the Palmqvist crack system, if it is more than 2.5, it is the radial median one. More than ten different equations exist, the most common are the following Equation 2:

$$K_{Ic} = 0.028 \cdot HV^{1/2} \cdot \left(\frac{F}{T}\right)^{1/2} \qquad \text{Palmqvist}$$

$$K_{Ic} = 0.0752 \cdot \frac{F}{c^{3/2}} \qquad \text{Evans and Charles}$$

Equation 2: (up) Palmqvist crack system equation, (down) Radial-median crack system with KIc the fracture toughness, HV the Vickers hardness (GPa), F the load applied (N), T the total crack length (m), c the crack length from the centre of the indentation to the crack tip (m) (Ćorić, Ćurković, & MajićRenjo, 2017).

d.Scratch test

i. Principle

The scratch test consists in measuring the penetration depth of a nano indenter with a known geometry in order to obtain the elastic-plastic properties of a material. The loaded tip is having a controlled movement on the sample surface. The load applied can be constant or dynamic, depending on the properties observed. This technic is usually applied for the characterisation of thin films. This method allows to learn about the cohesive/adhesive behaviour of a material and also to see the critical load before any damage on the surface.

ii. Constant load

With a constant load, two main indents are used, the Berkovich, a triangle-based pyramid or a spheric indent. The second one is preferred when the material is soft, is the load applied is low, it will show elastic deformation whereas if the load is bigger, elastic-plastic deformation will appear. The most commonly used is the Berkovich one, just because it is easier to design at that small size. (Caër, 2013)

iii.Increasing load

With an increasing load, the goal is to observe the limit load when a damage appears on the sample. The same Berkovitch tip can be employed. This increasing load method will be employed in our study, in order to create a damage.

iv.Execution

The device is made of an optical microscope, an indenter and a force senser. Various functions are available in order to scratch the surface and also to measure the topography. Three steps are involved in this measurement process:

- Measurement of the baseline profile “preprofile”
- Scratch step
- Measurement of the profile after the scratch and the plastic deformation

The measurement of the baseline profile is mandatory because the scratch can then be made with a corrected value taking into account the surface defects.

(Chapitre IV. Caractérisation de l’adhérence des couches minces par Scratch Test, 2013)

To analyse the results, various data can be used:

- The load applied along the scratch (blue line on the Figure 13)

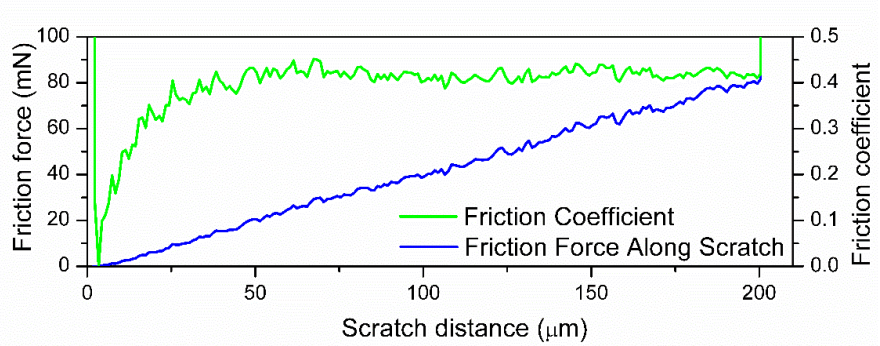

Figure 13: Friction force (mN) along the scratch (µm).

- The depth of the penetration along the scratch (red line on the Figure 14)

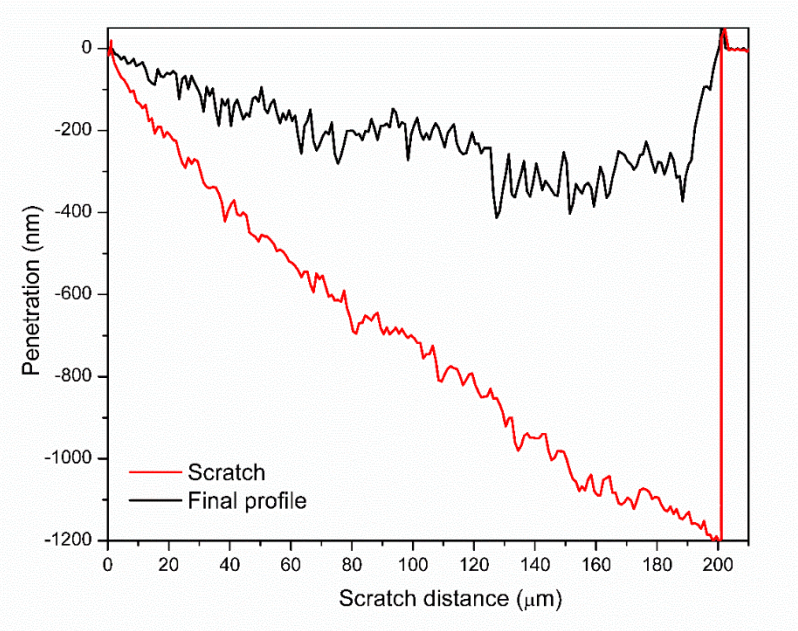

Figure 14: penetration depth (nm) along the scratch (µm).

- The final profile obtained by subtracting the baseline profile to the scratch profile (black line on the Figure 14)
- The SEM pictures (Figure 15), to compare the profile changes with the kind of cracks observed

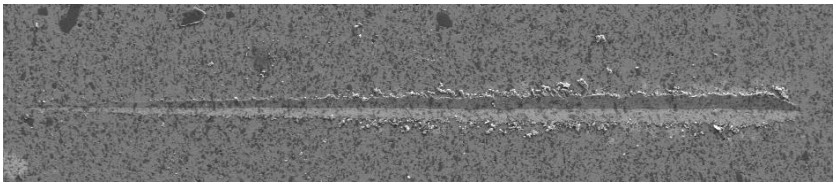

Figure 15: SEM pictures of the scratch produced by the tip during the test.

e.X-Ray Diffraction (XRD)

XRD is a non-destructive analysis technique, allowing to find the crystalline phases of a sample. The principle is quite simple, a monochromatic light is diffracted on the sample crystalline layers. The light is projected on the sample with an angle θ and a photons detector is placed in front of the incident light, with the same angle θ and set on the monochromatic source wavelength λ. (Figure 16: XRD schema)

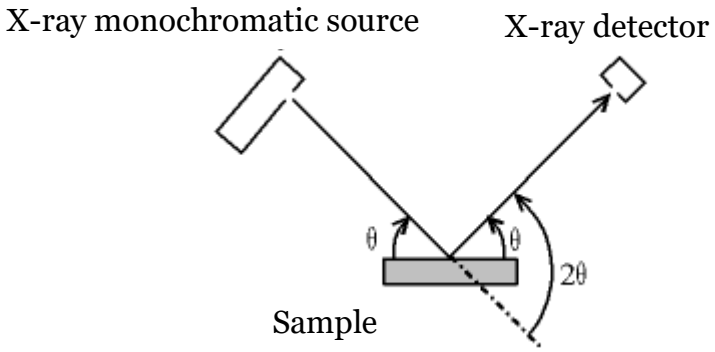

Figure 16: XRD schema.

If a Bragg condition is respected, it means if in the following equation n is an entire (Equation 3), most of the incident photons will diffract in direction of the detector.

$$2 \cdot d \cdot \sin\theta = n \cdot \lambda$$

Equation 3: Bragg's law.

With d the distance between two successive crystalline layers, θ the incidence angle, n an entire and λ the wavelength of the incident light.
The signal collected by the detector is transformed in a diffraction pattern as shown in the Figure 17.

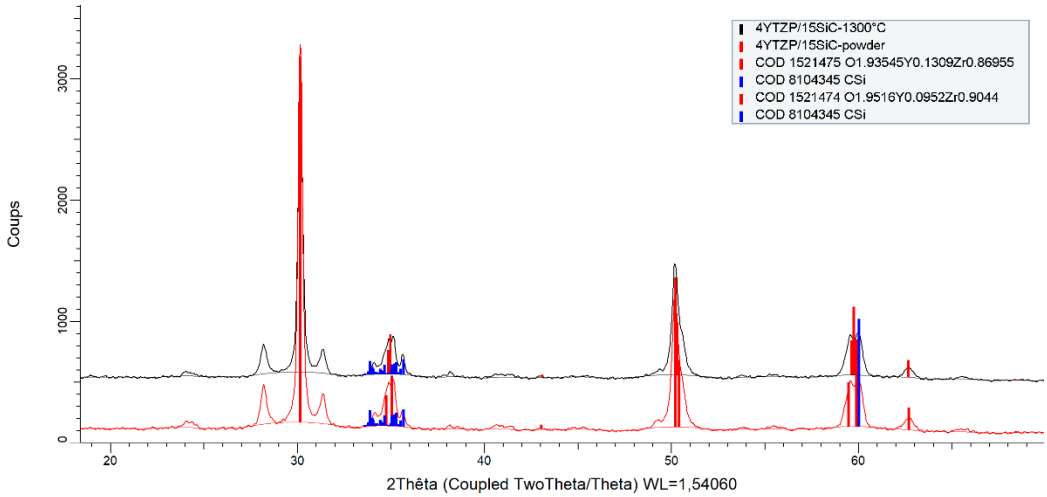

Figure 17: XRD diffraction pattern.

By studying the position of the peaks, one can find the crystalline phases, with the intensity, a quantitative analysis, and with the width, the size of the crystallites can be determined.

f.Field Emission Scanning Electron Microscopy (FESEM)

SEM functions as optical microscopy, at the exception that a focused ion beam replaced the light source to image the sample and obtain information about its structure and composition. It allows to have such a better magnification than traditional microscopes, so to see smaller objects. This, because the smallest the illuminating source wavelength is, the best the resolution.

The wavelength of the moving particles such as electrons is defined by Louis de Broglie by the following Equation 4:

$$\lambda = \frac{h}{mv}$$

Equation 4: De Broglie's law.

Where λ= wavelength of particles, h= Planck's constant, m= mass of the particle (electron), v= velocity of the particles.

5. Material characterisation

With the samples obtained by the SPS process, the ceramic can be characterized. For that, the following parts will detail each study made for the samples. First, the mechanical properties will be studied thanks to hardness and toughness information. Then, the composition of the samples, will be checked thanks to DRX patterns. To follow, the SEM pictures will inform on the fracture modes. Finally, the scratch test combined with thermal cycles, will give details on the material's behaviour at high temperature.

a.Hardness

The results obtained during the Vickers hardness indentation are presented on the following Figure *18*.

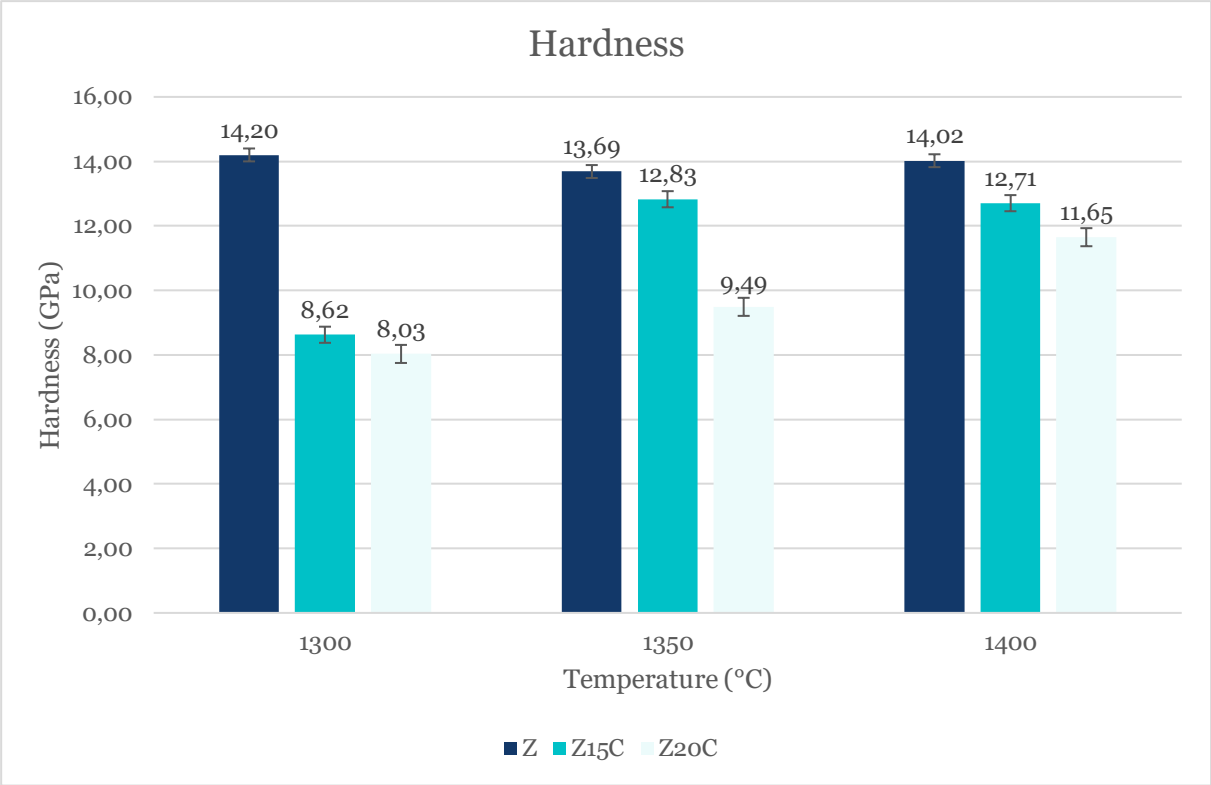

Figure 18 : Hardness values (GPA) as a function of the processing temperature (°C) for 3 materials.

The hardness values for the Zirconia (4YTZP) remain being the higher values. However, the values for the samples with SiC are showing that, to be fully sintered, and so harder, SiC needs to be heated much more than the zirconia alone, the sintering temperature of SiC is around 1800°C. Another observation is that when the SiC percentages in the composites increase, the hardness values decrease. Two main factors can act on the hardness values:

- The increase in the grain growth, that is proportional to the SiC particles quantity
- The low density of the materials

It means that if there is a big part of SiC in the material, the grains will be much bigger than at a lower temperature, and the hardness value will decrease.

One can see that the HV value for any sintering temperature is quite similar (13.69 – 14.2 GPa). The highest hardness values of the composites are obtained at 1350°C for the Z15C (12.83 GPa) and at 1400°C for the Z20C (11.65 GPa). Theoretically, the highest values would have been obtained for both composites at 1400°C, the difference between the Z15C hardness values at 1350°C and 1400 °C is very small, one can consider it is due to experimental approximations. In fact, the sintering temperature is not high enough to enables the SiC particles to sinter. Some additives can enter in the composition of the composite to decrease the needed sintering temperature, but in this project the choice has been made to keep the components without any additives. The values obtained during this project are similar to the values obtained in the (A. Borrell, 2020), values are compared in the Table 4.

Table 4 : comparative table for Vickers hardness values

	4YTZP (any temperatures)		**Z15C (1400°C)**		**Z20C (1400°C)**	
	Project	(A. Borrell, 2020)	Project	(A. Borrell, 2020)	Project	(A. Borrell, 2020)
Vickers hardness (GPa)	13.69-14.2	14.6-15.4	12.71	12.7	11.65	11.8

b.Fracture toughness

It is very important to deal with the fracture toughness because ceramics are brittle materials. Moreover, it is much more important for structural material, because they have to last in time, and not be broken at the first crack. On the following Figure 19, values of K_{IC} calculated thanks to Palmqvist Equation 2 are presented.

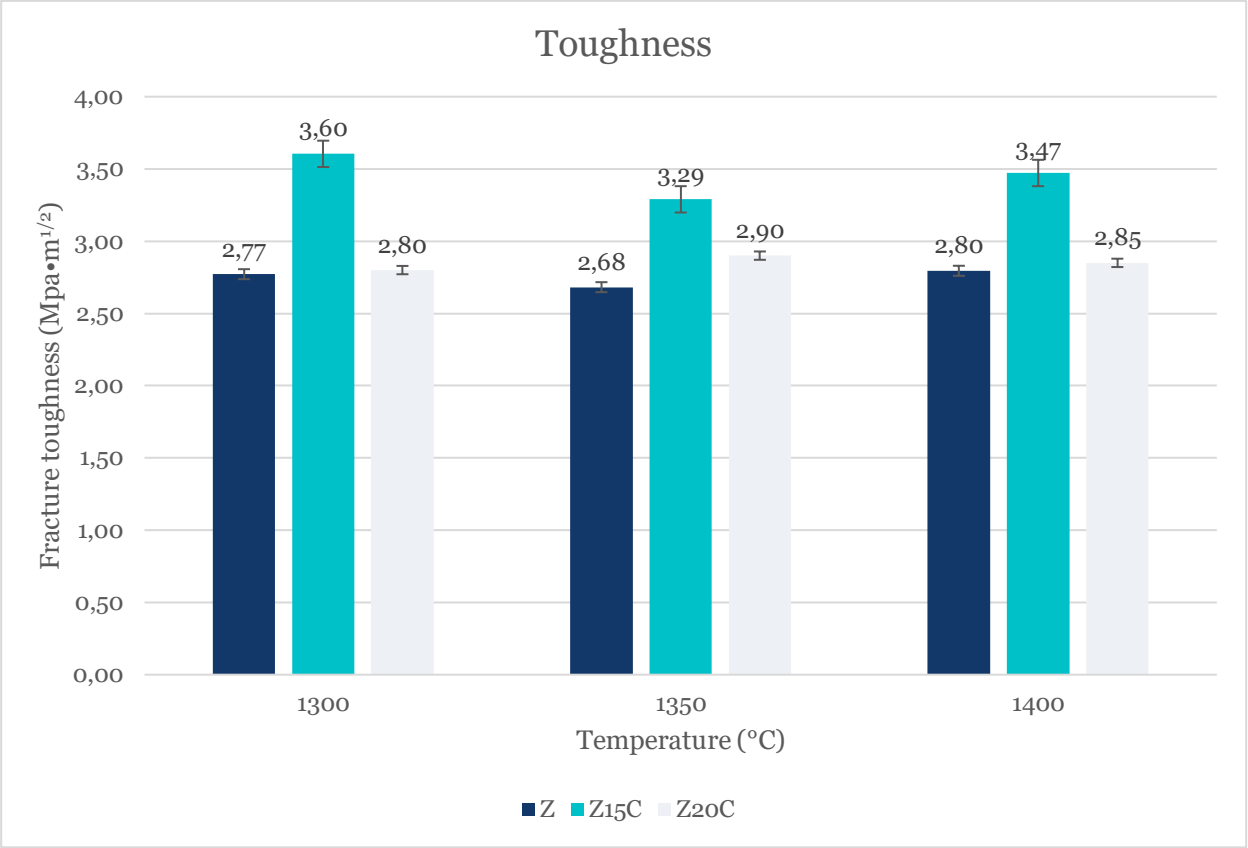

Figure 19 : Fracture toughness (MPa·$m^{1/2}$) as function of temperature (°C) for various materials.

One can see that the higher values of K_{IC} are obtained for the composites and not the 4YTZP, even if the values for Z20C are very close to 4YTZP ones. The best K_{IC} values are obtained with Z15C, with values between 3,29 and 3,60 MPa.$m^{1/2}$, the highest for 1300°C. Fracture toughness is, for TBCs applications, even more important than hardness, because it has to resist to temperature changes without crack propagation, that's why Z15C fits the best for TBCs applications.

c.XRD

The following Figure 20, Figure 21 and Figure 22 are the XRD patterns obtained for the three samples studied. The characteristic peaks of 4YTZP and SiC are represented respectively in red and blue. On the Figure 20, the visible peaks are the one corresponding to 4YTZP, the zirconia founded here is the tetragonal phase. There is no transformation to the monoclinic phase, thanks to the yttrium that stabilized the tetragonal phase.

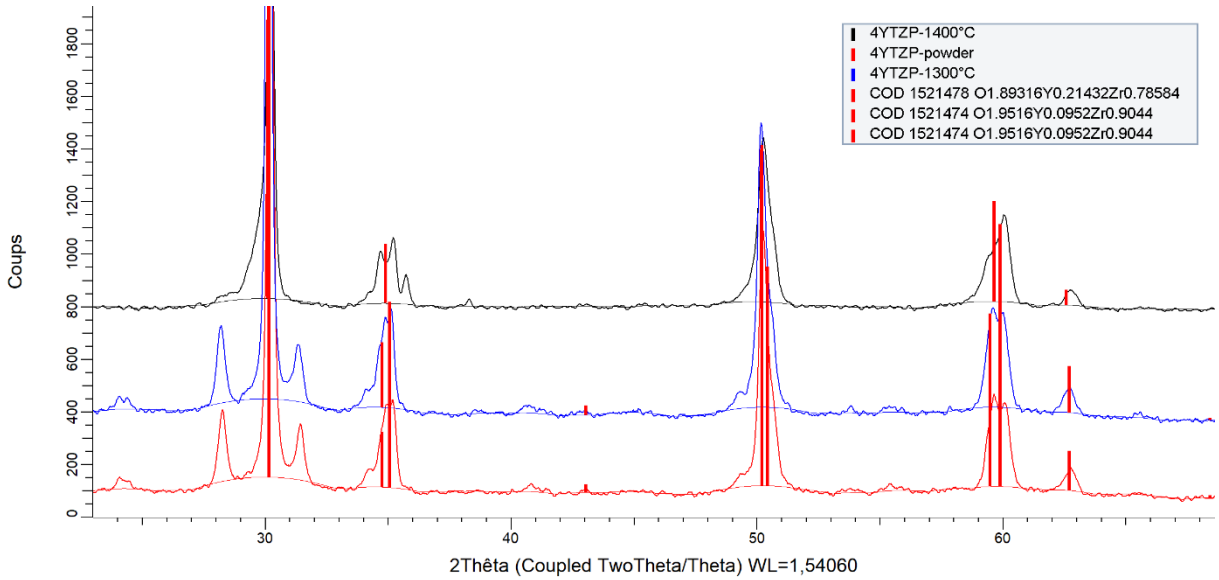

Figure 20: DRX pattern for 4YTZP samples.

On Figure 21 and Figure 22, the blue peaks corresponding to SiC overlap the 4YTZP peaks, indeed it means that by seeing the XRD pattern of 4TZP, it is not possible to determine if the sample is with or without SiC. One important things is to remark that there is no reaction between the 4YTZP and SiC, the patterns are really similar, leading to this conclusion.

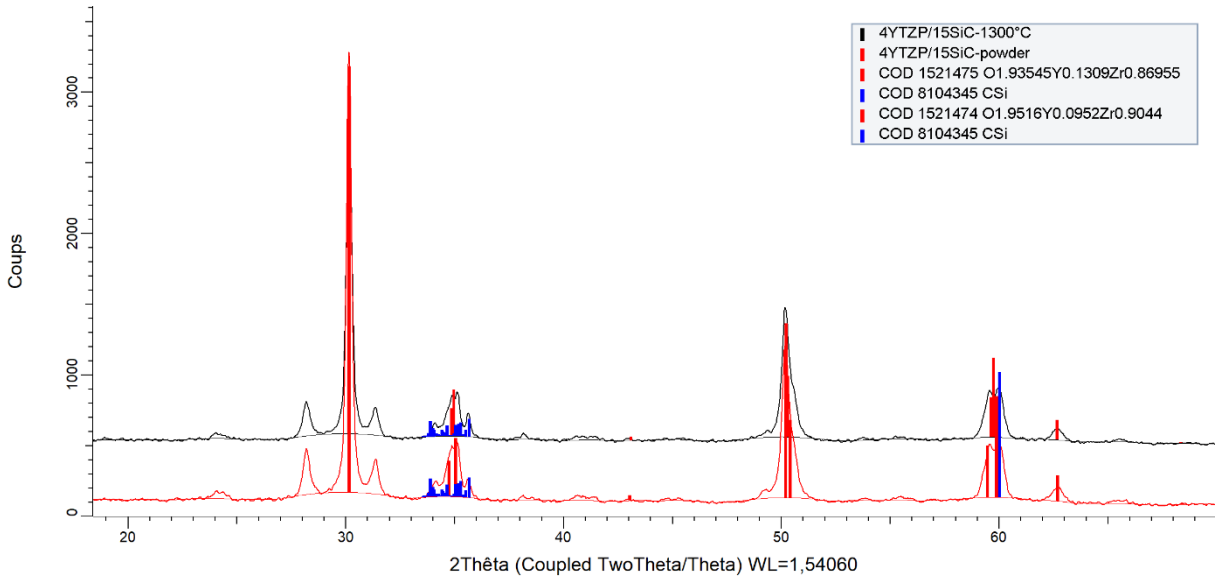

Figure 21: DRX pattern for 4YTZP/15SiC samples.

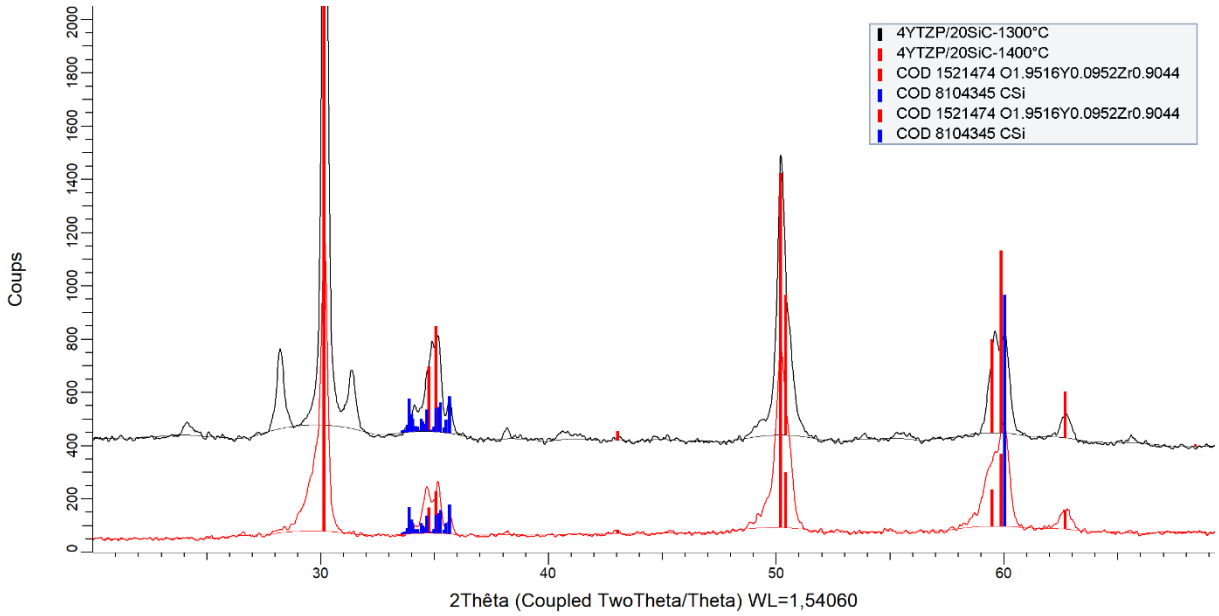

Figure 22:DRX pattern for 4YTZP/20Sic samples.

d.FESEM

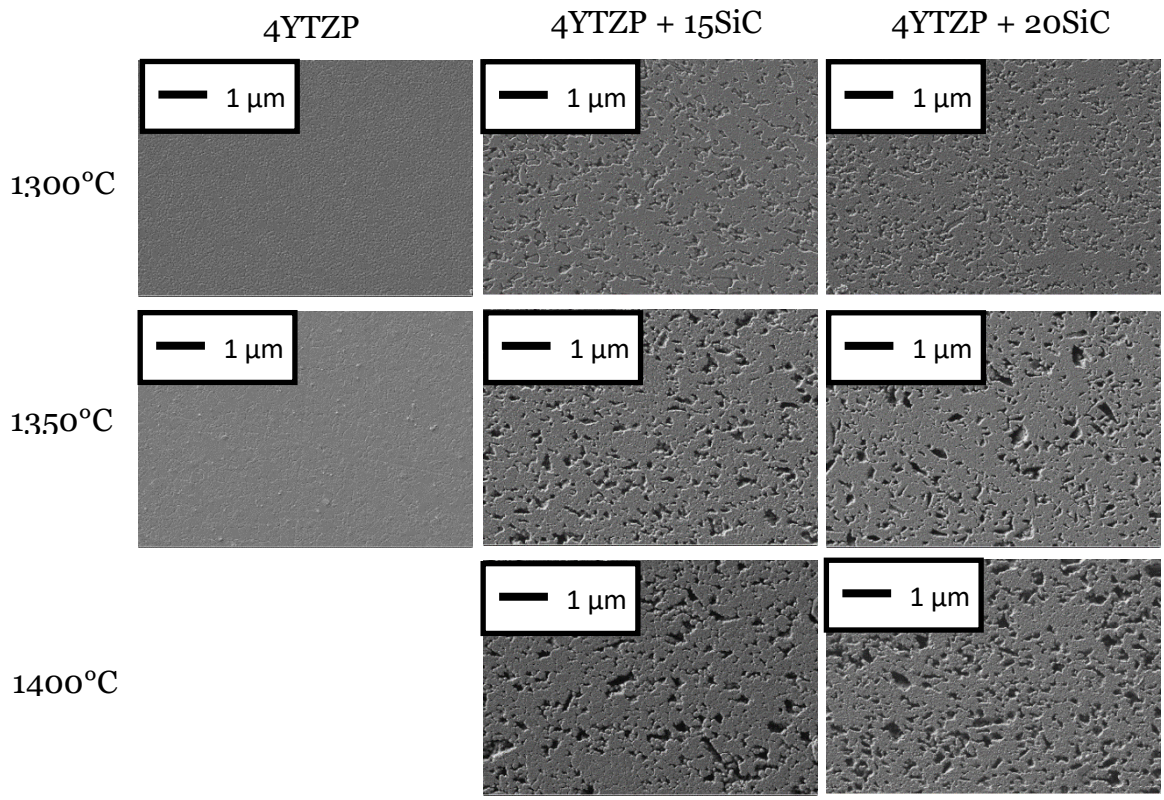

Figure 23 : SEM pictures of 4YTZP and composites (at the same scale) for the three temperatures studied.

SEM pictures of the polished surfaces of the samples are gathered on the Figure 23, one can see that the composite does not have a homogeneous structure, as the black inclusions are SiC particles. These particles are bigger at higher temperature because they grow with the heating. Unfortunately, the sintering temperature is not high enough to obtain a full densification of the composites

More than the simple polished surface, the fracture surface can give information about densification. The SEM micrographs of 4YTZP and SiC composites at 1350°C are presented on the Figure 24.

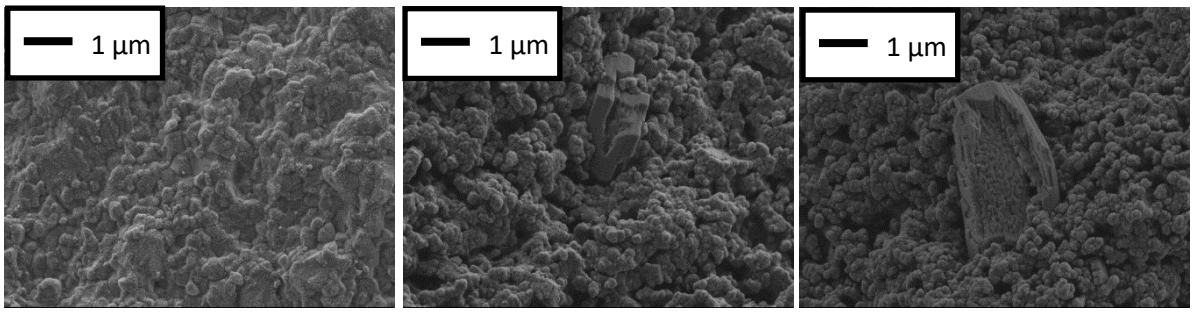

Figure 24 : SEM pictures of the fracture surfaces of 4YTZP, 4YTZP/15SiC and 4YTZP/20SiC at 1350°C.

It is possible to see that 4YTZP reaches full densification, no porosities can be seen on the SEM fracture surface picture, the sample seems to be homogeneous. On the contrary, the incomplete densification of the 4YTZP/15SiC and the 4YTZP/20SiC composites can be observed without taking into account the SiC proportion. SiC particles are clearly visible on the SEM pictures, they are not integrated to the matrix, and the SiC grains are much bigger than the 4YTZP grains, leading to the creation of pores.

In order to check if the composites can really be employed as TBCs materials, samples containing cracks where placed during 1 h in an oven at 1000°C, the result is Figure 25.

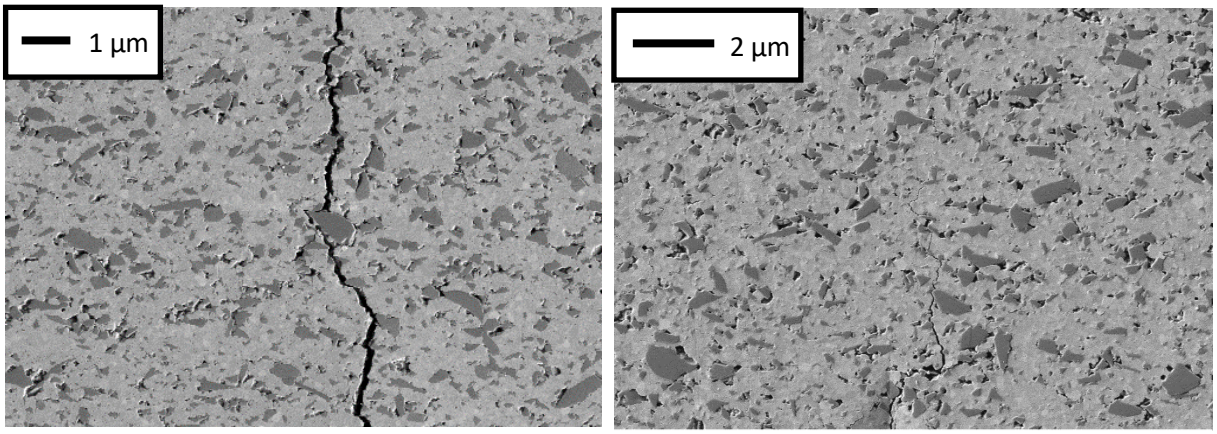

Figure 25 : SEM pictures of 4YTZP/15SiC (left) with a crack (right) after 1h at 1000°C.

The difference between the thermal expansion coefficient of the matrix and the SiC, creates pores and can also break particles. This creates cracks, but it is also this difference in expansion coefficient that allows pores to act as cracks inhibitor.

e.Scratch test

A scratch test was made for each sample at 1300°C and 1400°C, the results are the followings.

- 4YTZP – 1300°C

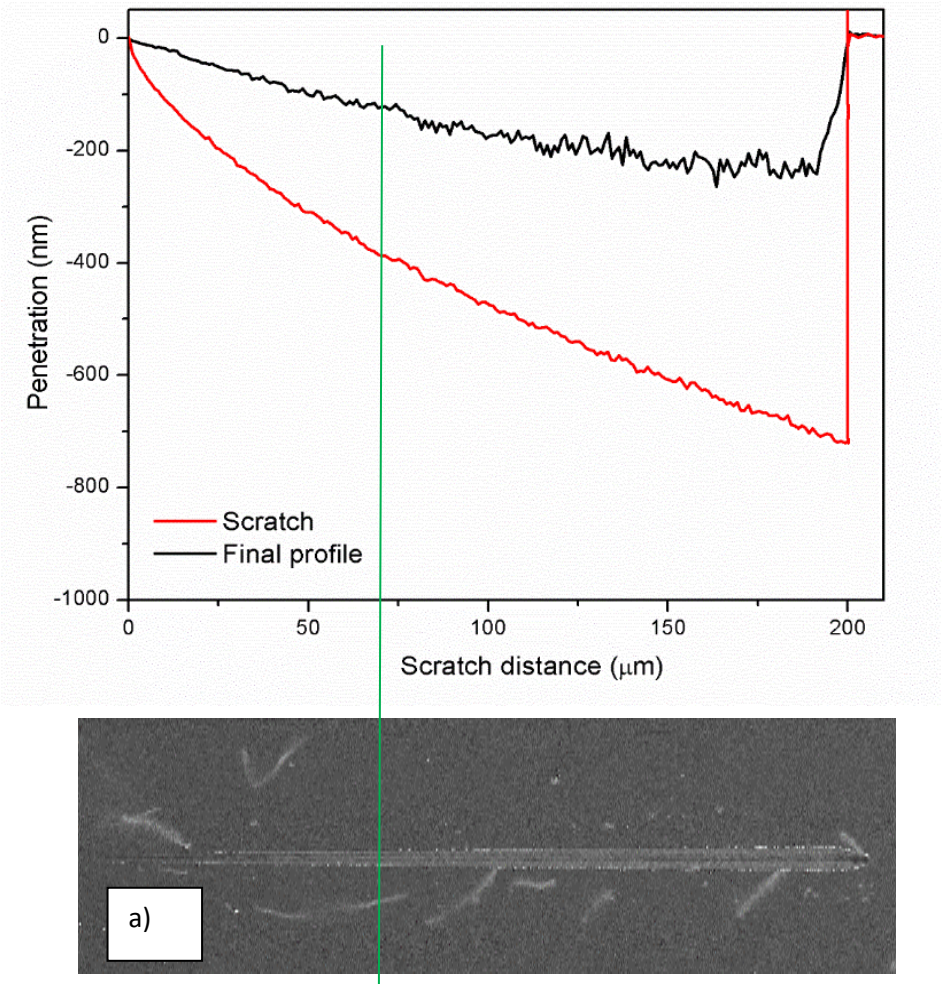

Figure 26 : Scratch test graph, associated picture for 4YTZP-1300°C.

On the Figure 26 the scratch distance is corresponding on the graph and on the picture a), the line of the final profile starts to have more relief around 75µm after the beginning of the scratch test, when a certain depth is reached, the grains start to have more movement.

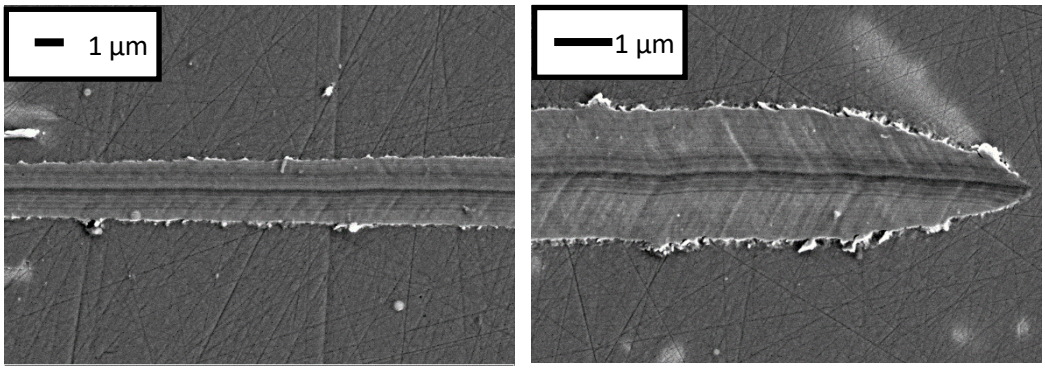

Figure 27 : pictures of the scratch on 4YTZP-1300°C sample.

On the left of the Figure 27, one can see irregularities appearing at the border between the scratch and the rest of the sample. By taking a closer look (right picture), herringbones are visible, on the opposite direction as the movement. This means that the sample is subjected to tensile stress.
On can see white marks around the scratch, they may be the result of internal cracks created by the tensile stress, because ceramic do not have good tensile strength.

- 4YTZP-1400°C

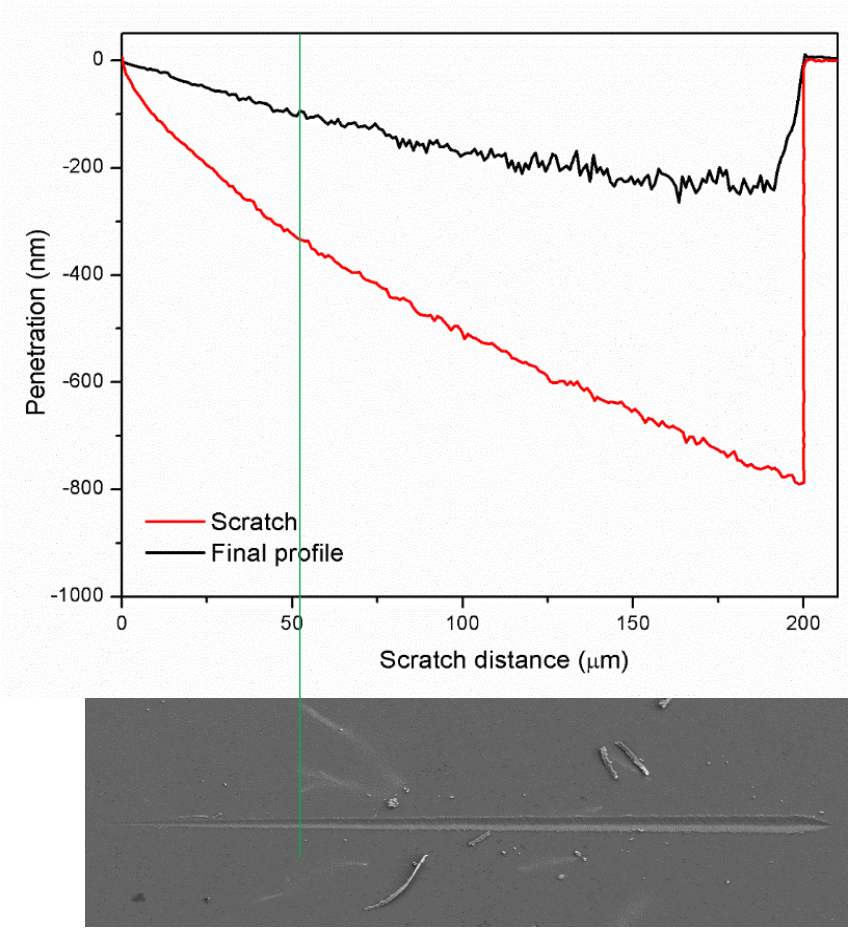

Figure 28 : Scratch test graph and associated pictures 4YTZP-1400°C

As with sintered samples at 1300°C, 4YTZP-1400°C exhibits herringbone as soon as grain detachment is observed, it means after the green line (Figure 28). The white marks also remain. The biggest difference is the depth of penetration, using the same friction force along the scratch, the tip is deeper in the 4YTZP-1400°C. That means that the 4YTZP-1400°C has a hardness values lower than 4YTZP-1300°C, with the results obtained on the Figure *18*, the results are coherent.

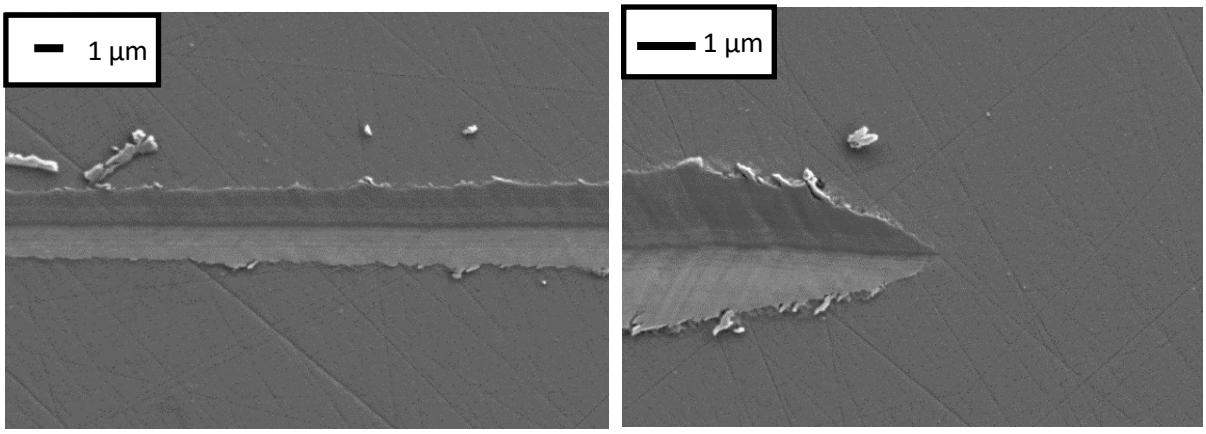

Figure 29 : pictures of the scratch for the 4YTZP-1400°C sample.

- 4YTZP/15SiC-1300°C

On Figure *30* are presented the result for the composite 4YTZP/SiC-1300°C. The depth of penetration is much larger than for 4YTZP, the composite has indeed lower values of hardness than the matrix alone. Once again, this result is consistent with the hardness values obtained previously. This is because the composites are not as dense as the matrix because the SiC has not reached a sufficient temperature to be sintered completely during the SPS process.
One can remark, in the image on the right, that the greater the depth of the scratch, the greater the size of the debris around it. These debris might be big grains or grains agglomerates.

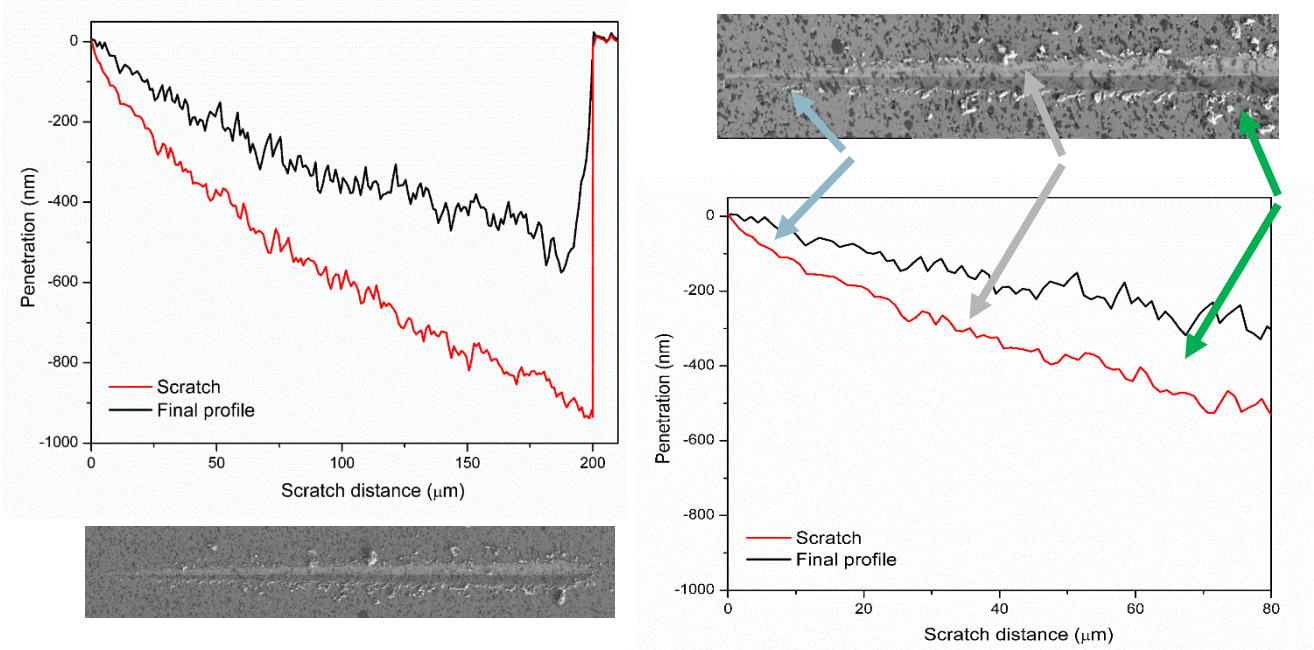

Figure 30 : Scratch graph and associated pictures (left), with a larger zoom (right) for 4YTZP/15SiC 1300°C.

- 4YTZP/15SiC-1400°C

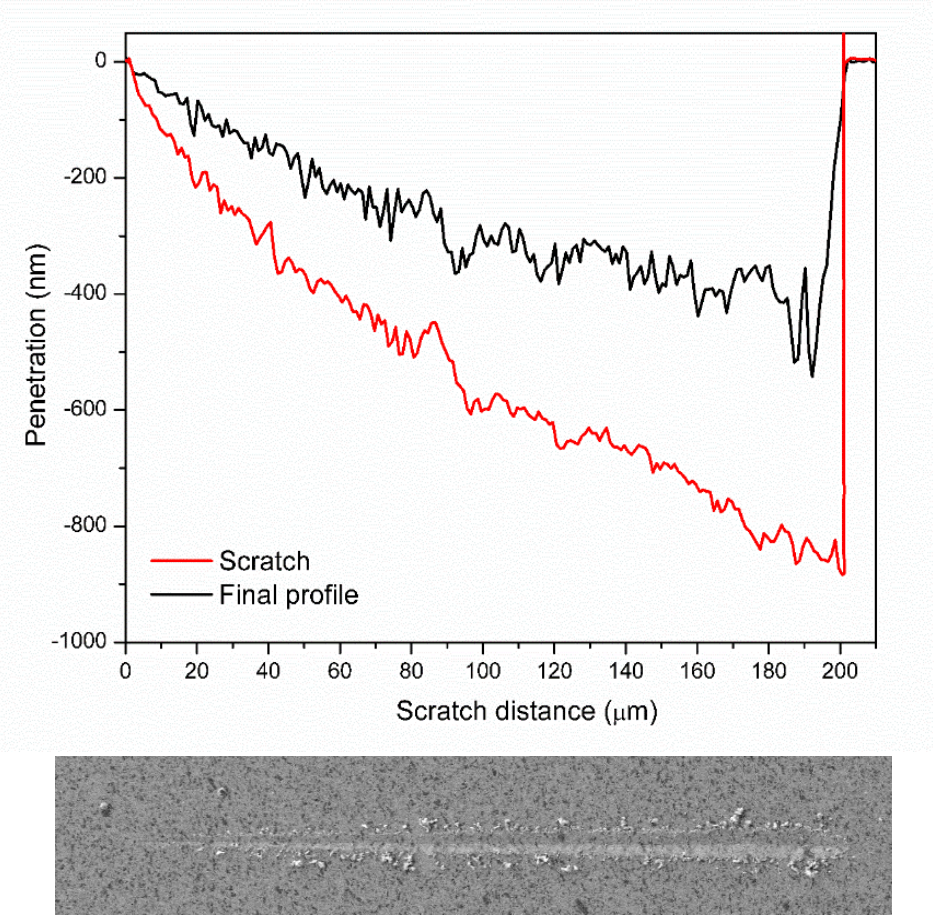

Figure 31 : Scratch test graph and associated picture for 4YTZP/15SiC-1400°C.

For 4YTZP/SiC sintered at 1400°C, the depth of penetration (Figure *31*) is a bit lower than for 1300°C, showing better hardness value. On the Figure *32*, on the left, cracks are visible, they might be a result of tensile stress created by the force applied on the tip. On the right picture, SiC grains are black and they show major defects, their surface is not flat, they have been damaged by the tip.

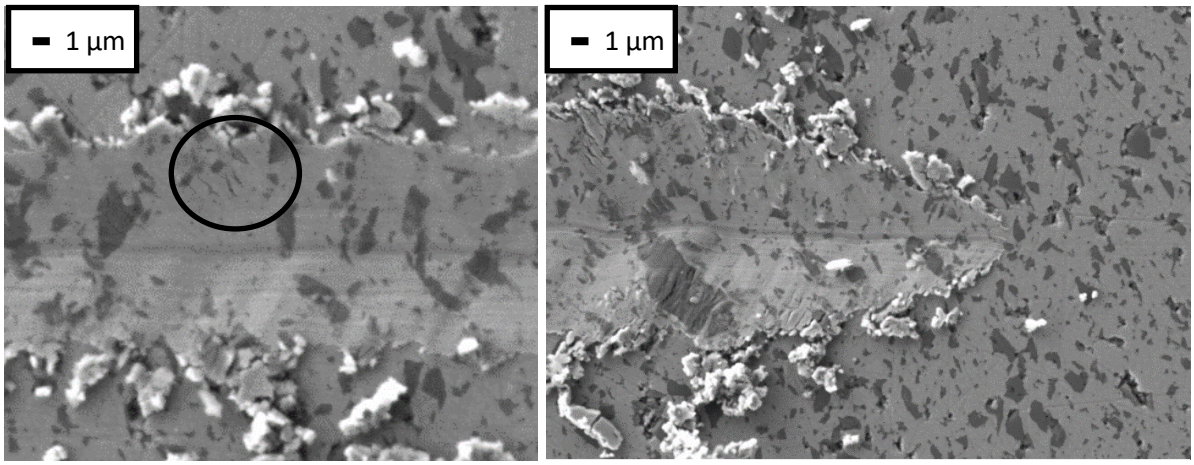

Figure 32 : pictures of the scratch for 4YTZP/15SiC-1400°C.

- 4YTZP/20SiC-1300°C

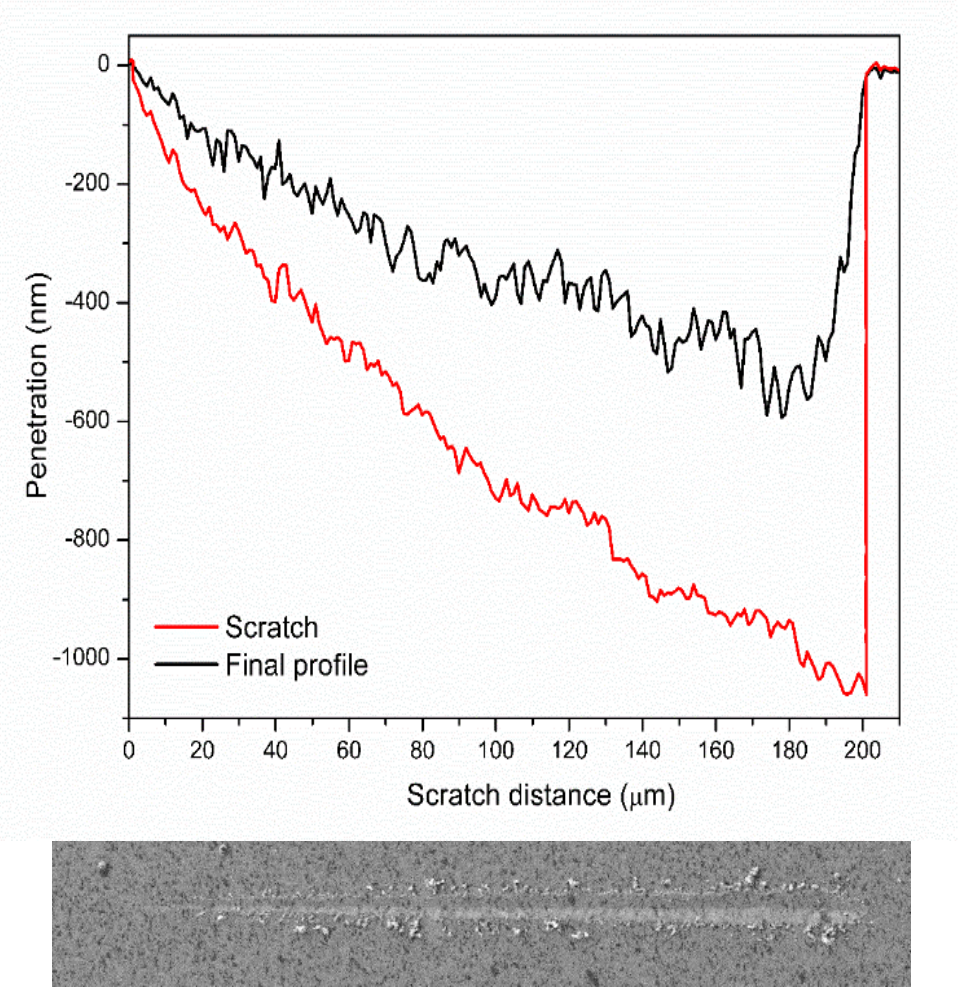

Figure 33:Scratch test graph and associated picture for 4YTZP/20SiC-1300°C

As shown on Figure 33*:Scratch test graph and associated picture for 4YTZP/20SiC-1300°C*, the penetration depth is bigger than for the earlier composite 4YTZP/15SiC, meaning a lower hardness value. Defects and cracks are again clearly visible on the picture Figure 34 *: picture of the scratch on the 4YTZP/20SiC-1300°C*

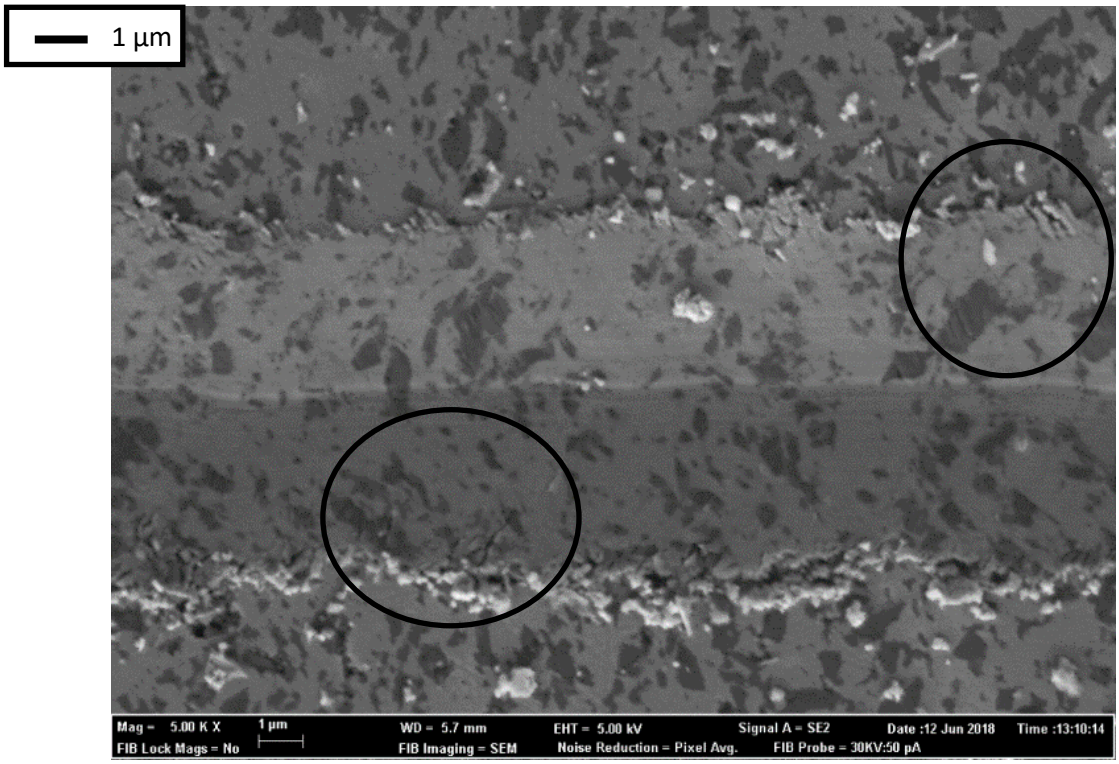

Figure 34 : picture of the scratch on the 4YTZP/20SiC-1300°C.

- 4YTZP/20SiC-1400°C

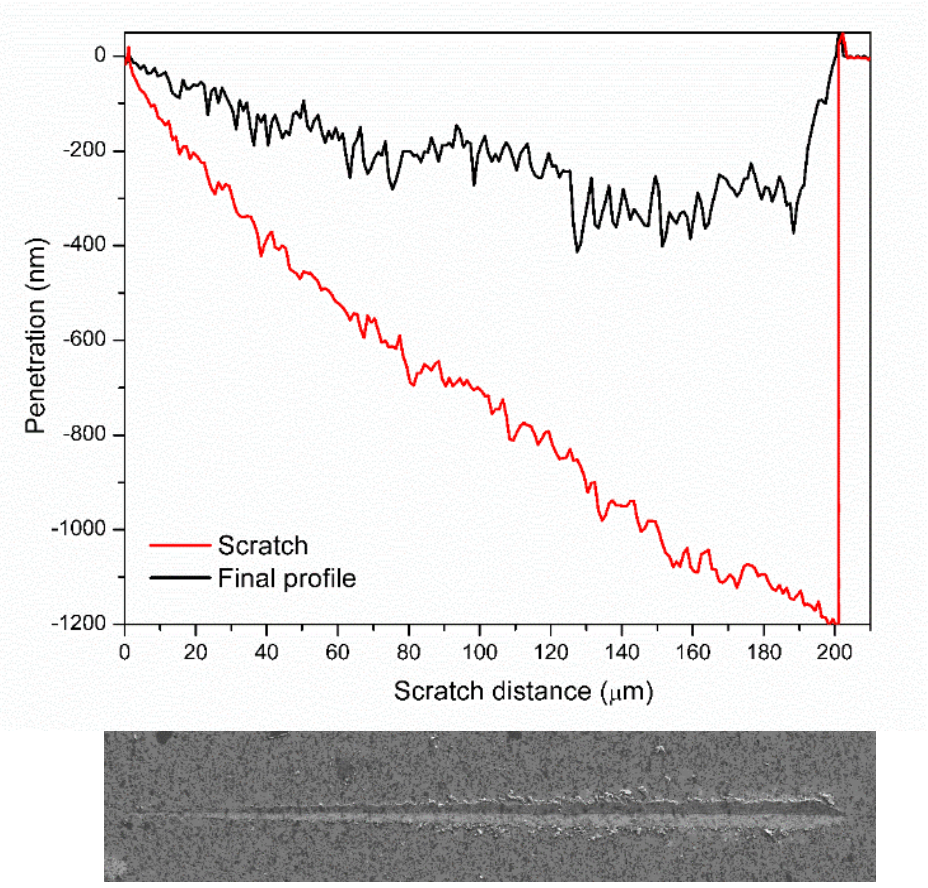

Figure 35 : scratch test graph and associated pictures for 4YTZP/20SiC-1400°C.

Comparing the Figure 35 to the Figure 33, the depth penetration is even bigger, this is not consistent with the results obtained on the Figure 18, where the hardness value was higher for the 4YTZP/20SiC sintered at 1400°C than the one sintered at 1300°C. The samples are not homogeneous because the SiC is not fully sintered, maybe, while doing multiple scratch tests, better result could have been obtained.

6. Conclusion

In order to determine SiC effects on a Zirconia-based matrix, mechanical properties and microstructure of SPS sintered composites were studied. With SiC particles and sintering temperature between 1300°C and 1400°C, the composites can be fully densified. Moreover, they create an increase on the 4YTZP grain size, leading to a less homogeneous microstructure. As shown with the XRD results, there is reaction between 4YTZP and SiC, this material is an accurate reinforcement. The composite 4YTZP/15SiC has the best fracture toughness at any sintering temperature, it means that adding more SiC is not necessary to enjoy the mechanical benefits of its structure.

7. Recommendation for future work

For future work about 4YTZP based composites, it would be interesting to study the properties of a composites made of 4YTZP/SiC and SiO2. The silicon oxide (SiO2) is supposed to improve the fracture toughness of the material, helping the material to act as a crack inhibitor.
It could also be informative to know how these materials would act at high temperature. Cracks have been seen after the scratch test; they may disappear after a heating process. This could confirm again the use of 4YTZP/SiC composites on TBCs application.

8. Project budget

The prices of the equipment employed to achieve this project are gathered on Table 5. The amortization time of such equipment is 10 years, but one part of them is already amortized because they remain being at the ITM (Instituto Tecnológico de Materiales) for more than 10 years. Therefore, to realize this project, a previous investment of 312 075€ was necessary.

Table 5 : prices equipment ITM.

Equipment	***Quantity***	***Price (€)***
Colloidal Processing and Freeze-Drying	1	40500.00
Laser Particle Size Analyzer and Computer Equipment	1	32000.00
Spark Plasma Sintering	1	35000.00
Heating plate with magnetic stirrer	1	325.00
Precision analytical balance and density measurement equipment	1	8000.00
Thread cutter *Stuffer* *Polishing machine with lapping discs*	1	63000.00
Microdurometer and Computer Equipment	1	22900.00
Optical Microscope and Computer Equipment	1	80000.00
Drying Stove	1	2350.00
Oven	1	28000.00
Total		**312075.00**

a. Measurements

This section contains the estimated measurements of human resources(Table 6 *: Human resources estimation*), electrical energy consumption (Table 7), tools and products employed (Table 8, Table 9) and laboratory technical services (Table 10) which have been used for the implementation of the project. It is important to note that the samples were already prepared and sintered, and were already used for other projects, equally, raw data of previous results have been employed because of the incapacity to go physically at the laboratory to process the experiment due the sanitary conditions (COVID-19).

Table 6 : Human resources estimation.

Person	***Unity***	***Quantity***
Project director	h	54
Laboratory technician	h	32

Table 7 : Energy consumption.

Device	***Power specifications (W)***	***Estimated hours of use (h)***	***Unity***	***Quantity***
Cutting device	750	5	kW h	3.25

Stuffer	1000	4	kW h	4.00
Polishing device	570	10	kW h	5.70
Microdurometer + computer equipment	150	15	kW h	2.25
Optical microscope + computer equipment	320	15	kW h	4.8
Drying oven	1600	5	kW h	8.00
Oven	4500	38	kW h	171.00
Total			**kW h**	**197**

Table 8 : Tools employed.

Tool	***Reference quantity***	***Quantity***
Beakers 100 mL	Ud	3
Pipette	Ud	1
Metal clamps	Ud	1
Metal spatula	Ud	1
Plastics boxes	Ud	1
Latex gloves box	Ud	1
Polishing plates	Ud	7

Table 9 : Products consumption.

Products	***Reference quantity***	***Quantity***
4YTZP	g	1000
SiC	g	1000
Distilled water	mL	2000
Ethanol	mL	500
Abrasive (diamond paste)	mL	500
Stamping resin	g	210

Table 10 : laboratory technical services.

Service	***Reference quantity***	***Quantity***
Electronic microscopy service of the Universidad Politècnica de València. FE-SEM equipment. Including sample preparation material.	h	10
X-ray SCSI service. UPV agreement with UV. Phase identification.	sample	21

b.**Unit price tables**

This section provides tables of unit prices for human resources (Table 11), electrical energy consumption (Table 12), tools and products employed (Table 13, Table 14) and the technical services (Table 15).

Table 11 : unit prices for human resources.

Person	*Reference quantity*	*Price (€)*	*Unit price (€ ud^{-1})*
Project director	1	24.00	24.00
Laboratory technician	1	12.30	12.30

Table 12 : unit price of energy.

	Reference quantity	*Price (€)*	*Unit price (€ ud^{-1})*
Kilowatt-hour	1	0.0855	0.0855

Table 13 : Unit prices of the products.

Product	*Reference quantity*	*Price (€)*	*Unit price (€ ud^{-1})*
Beakers 100 mL	1	0.96	0.96
Pipette	1	0.80	0.80
Metal clamps	1	2.55	2.55
Metal spatula	1	2.89	2.89
Plastic box	1	0.82	0.82
Latex gloves box	1	4.39	4.39
Polishing plates	1	200.00	200.00

Table 14 : Unit prices of the components.

Products	*Reference quantity*	*Price (€)*	*Unit price (€ ud^{-1})*
g of 4YTZP	1000	134.20	0.134
g of SiC	1000	120.90	0.121
mL of distilled water	5000	10.92	0.002
mL of ethanol	5000	78.16	0.016
mL of abrasive diamond paste	1000	160	0.16
mg of stamping resin	2300	200	0.087

Table 15 : technical services unit prices

Technical service	*Reference quantity*	*Price (€)*	*Unit price (€ ud-1)*
Electronic microscopy service of the Universidad Politècnica de València. FE-SEM equipment. Including sample preparation material.	1	20	20
XRD Sample.	1	8	8

c. Partial budget

Table 16 : partial budget: human resources

Person	*Quantity*	*Unit price (€ ud^{-1})*	*Price (€)*
Project director	54	24.00	1296
Laboratory technician	32	12.30	393

Table 17 : partial budget: energy consumption

	Quantity	*Unit price (€ ud^{-1})*	*Price (€)*
Kilowatt-hour	197	0.0855	16.85

Table 18 : partial budget: products

Product	*Quantity*	*Unit price (€ ud^{-1})*	*Price (€)*
Beakers 100 mL	3	0.96	2.88
Pipette	1	0.80	0.80
Metal clamps	1	2.55	2.55
Metal spatula	1	2.89	2.89
Plastic box	1	0.82	0.82
Latex gloves box	1	4.39	4.39
Polishing plates	7	200.00	1400

Table 19 : partial budget: Components

Component	*Quantity*	*Unit price (€ ud^{-1})*	*Price (€)*
g of 4YTZP	1000	0.134	134
g of SiC	1000	0.121	121
mL of distilled water	2000	0.002	4
mL of ethanol	500	0.016	8
mL of abrasive diamond paste	500	0.16	80
mg of stamping resin	210	0.087	18.27

Table 20 : partial budget: technical services

Technical service	***Quantity***	***Unit price (€ ud^{-1})***	***Price (€))***
Electronic microscopy service of the Universidad Politècnica de València. FE-SEM equipment. Including sample preparation material.	10	20	200
XRD Sample.	21	8	168

d. Total budget of the project

The Table 21 shows the total estimated budget for this TFM. It only includes items with a known value.

Table 21: total budget

	Price (€)
Human resources	1689
Products	1414.33
Components	365.27
Energy consumption	16.85
Technical services	368
Total (without taxes)	3853.45
Total (21% taxes included)	**4662.67**

9. References

A. Borrell, e. a. (2020). *Microstructure and mechanical properties of 4YTZP-SiC composites obtained through colloidal processing and Spark Plasma Sintering.* Bol. Soc. Esp. Cerám. Vidr.

Bichaud., E. (2016). *Frittage " flash " de céramiques sous courant alternatif.* Université Grenoble Alpes.

Borrell Tomás, M., & Salvador Moya, M. (2018). *Materiales cerámicos avanzados:.* Valencia: Editorial Universitat Politècnica de València.

Butler, E. P. (1985). *Transformation-toughened zirconia ceramics.* Materials Science and Technology.

Caër, C. (2013). *Caractérisation par nanoindentation et modélisation micromécanique de l'activation de mécanismes inélastiques : plasticité cristalline et transformation martensitique.*

Chapitre IV. Caractérisation de l'adhérence des couches minces par Scratch Test. (2013). Récupéré sur institut numérique: https://www.institut-numerique.org/chapitre-iv-caracterisation-de-ladherence-des-couches-minces-par-scratch-test-519f4d00903d5/amp

Chougrani, K. &. (2020). *Detection of Transparent Cracks Using Nonlinear Acoustics. .*

Ćorić, D., Ćurković, L., & MajićRenjo, M. (2017). *STATISTICAL ANALYSIS OF VICKERS INDENTATION FRACTURE TOUGHNESS OF Y-TZP CERAMICS.*

ESTOURNES, C. (2006). *Mise en forme de matériaux par frittage flash.* Mécanique | Travail des matériaux - Assemblage.

Faraji, G., Kim, H. S., & Kashi, H. T. (2018). *Mechanical Properties of Ultrafine-Grained and Nanostructured Metals.* Severe Plastic Deformation.

Kelly, J. R. (2007). *Stabilized zirconia as a structural ceramic: An overview.*

Miller, R. A. (1987). *CURRENT STATUS OF THERMAL BARRIER.* National Aeronautics and Space Administration, Lewis Research Center, Cleveland, OH.

Miller, R. A. (1997). *Thermal Barrier Coatings for Aircraft Engines: .* Journal of Thermal Spray Technology.

Moustabchir, H. (2008). *Etude des défauts présents dans des tuyaux soumis à une pression interne.* Université Paul Verlaine - Metz.

RAYNAUD, C. (2007). *Propriétés physiques etélectroniques du carbure de silicium (SiC).* Énergies | Conversion de l'énergie électrique.